Progress In Electromagnetics Research Letters, Vol. 107, 59–66, 2022

Asymmetric Coplanar Strip-Fed Electrically Small Metamaterial Inspired Antenna for Quadband Operation

Prathibha N. Pillai* and Ramasamy Pandeeswari

Abstract—This article presents a novel electrically small asymmetric coplanar strip (ACS) fed metamaterial inspired antenna for quad band operation. A metamaterial inspired open split ring resonator (OSRR) is the radiator which is fed using ACS to obtain four operating bands. The proposed antenna with a compact size of 18 mm × 15.5 mm × 1.6 mm is fabricated and tested. The experimental results are in good compliance with simulated ones. The proposed electrically small antenna has a radian sphere (ka) of 0.65 and achieves an average gain of 2.24 dBi with requisite radiation properties suitable for WiMAX and WLAN applications.

1. INTRODUCTION

Recent advancements in wireless communication demand the integration of numerous communication devices in a single module. Compact antennas with multiband operation are needed for such applications. Electrically small antenna (ESA) has immense prospects due to its multiband characteristics, small size, and ease of integration [1, 2]. Achieving a trade-off among impedance matching, gain, bandwidth, and radiation efficiency is challenging for ESA designs [3]. Metamaterial (MTM) loading has emerged as a novel approach in ESA design [4, 5]. Metamaterials are artificially generated electromagnetic structures having properties not seen in natural materials [6]. MTM structures are employed in MTM inspired antennas, filters, sensors, and absorbers for performance enhancement and miniaturization [7–9]. Further miniaturization is made possible by making use of ACS feed which reduces the antenna size to almost half of that of coplanar waveguide designs [10]. Many multiband antennas with ACS feed can be seen in literature [11–13]. Also, numerous ESA designs have been reported which are less compact, having less gain or with fewer operational bands than required.

This work focuses on the design of an ACS-fed electrically small antenna for quad band operation with a metamaterial inspired structure. The antenna has a compact size of 18 mm × 15.5 mm × 1.6 mm with an average gain of 2.24 dBi. Section 2 of the article discusses the design configuration. The results of design analysis are discussed in Section 3. The extraction of negative permeability of OSRR is detailed in Section 4. The concluding remarks are made in section 5. All simulations are done using Ansys HFSS software.

2. DESIGN CONFIGURATION

The proposed antenna has evolved to its final configuration through four stages as depicted in Figure 1(a). The design commences with an ACS-fed OSRR with one ring of size $15.5 \times 18 \times 1.6\,\text{mm}^3$ which yields a single resonance at 4.2 GHz. In stage 2, the radiator is an OSRR with two rings. This generates four resonances at 2.45 GHz, 3.65 GHz, 4.7 GHz, and 5.9 GHz. A third inner ring is introduced

Received 6 September 2022, Accepted 14 October 2022, Scheduled 25 October 2022
* Corresponding author: Prathibha N. Pillai (pnprathibha@gmail.com).
The authors are with the National Institute of Technology, Tiruchirappalli, India.

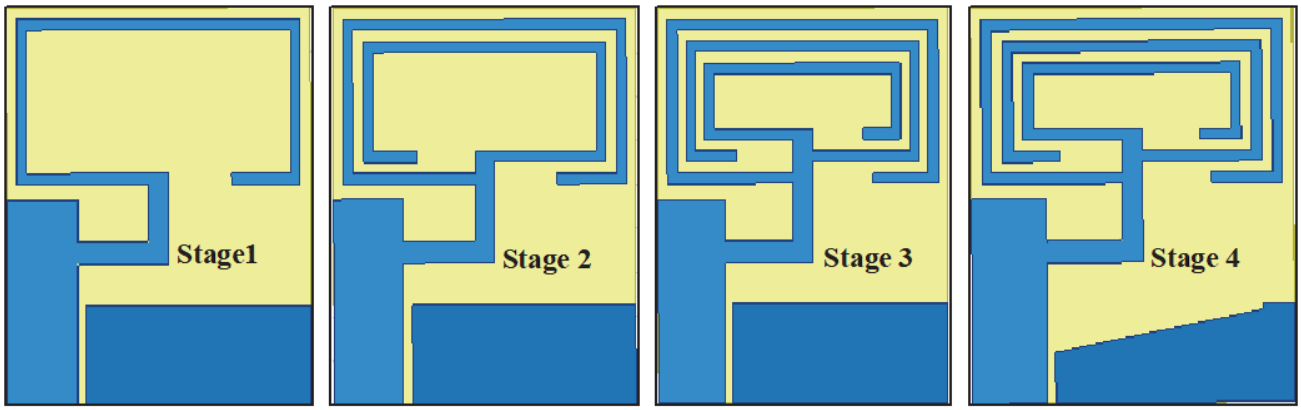

(a)

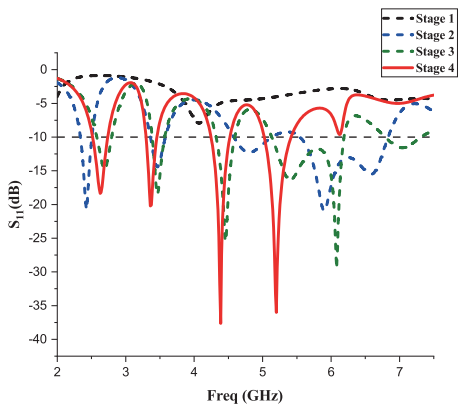

(b)

Figure 1. (a) Evolution of proposed antenna. (b) Simulated return loss S_{11} of evolution stages.

in stage 3 which yields resonances at 2.75 GHz, 3.65 GHz, 4.5 GHz, and 6.1 GHz and also improves the impedance matching. The final stage incorporates a modified ground plane resulting in resonances in the required operational frequencies of 2.64 GHz, 3.36 GHz, 4.38 GHz, and 5.2 GHz with better impedance matching. The return loss characteristics of these four stages are depicted in Figure 1(b). The antenna is fabricated using an FR-4 substrate possessing a relative permittivity of 4.4 and substrate thickness of 1.6 mm. The designed antenna has a compact volume of 446.4 mm^3. The antenna configuration with its design parameters is detailed in Figure 2(a). Figure 2(b) presents the equivalent circuit of the antenna. Here L_1 represents the electrical length of a microstrip line, Z_0 the characteristic impedance, and R the loss in the feedline. Each RLC network in the equivalent circuit corresponds to each resonating frequency, which is 2.64 GHz, 3.36 GHz, 4.38 GHz, and 5.2 GHz. The simulated and circuit model responses of the proposed antenna are shown in Figure 2(c).

For an antenna to be electrically small, the radian sphere $ka < 1$ where k is the free space wave number and a the radius of the sphere encompassing maximal dimension of antenna in meters. Here the sphere refers to the hypothetical sphere of minimum radius, a, that encloses the antenna to which an electrically small antenna must diminish its fields. For the proposed antenna, wave number k is 55.3 rad/m, and a is 0.0118 m for an operational frequency of 2.64 GHz. Hence the calculated value of ka equals 0.652 which is less than unity and thereby classifies this proposed ACS-fed design as an electrically small antenna. The maximum bandwidth and achievable Q of the antenna are 13.5% and 5.14%, respectively.

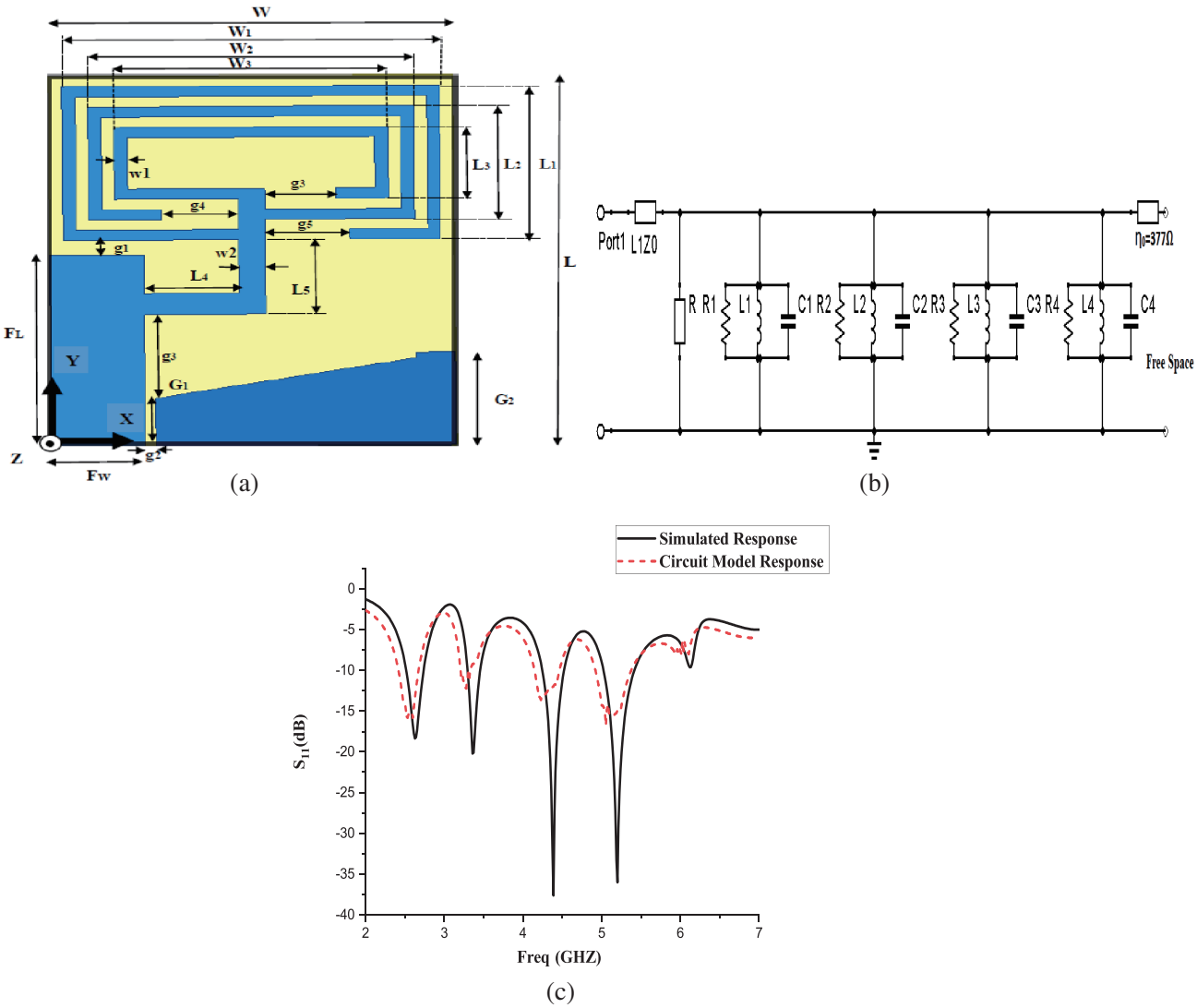

Figure 2. (a) Design dimensions of proposed antenna (in mm), $L = 18$, $W = 15.5$, $F_L = 9.3$, $G_1 = 2.3$, $G_2 = 4.5$, $F_W = 3.6$, $g_1 = 0.7$, $g_2 = 0.4$, $g_3 = 2.75$, $g_4 = 3$, $g_5 = 3.25$, $L_1 = 7.5$, $L_2 = 6.5$, $L_3 = 5.5$, $L_4 = 3.65$, $L_5 = 3.6$, $w_1 = 0.5$, $w_2 = 1$, $W_1 = 14.5$, $W_2 = 12.5$, $W_3 = 10.5$. (b) Equivalent circuit of antenna. (c) Simulated and circuit model response of antenna.

3. RESULTS AND DISCUSSION

The geometrical parameters of the proposed antenna are affirmed based on parametric analysis. The geometry of the ground plane is optimized based on current distribution. The leading edge of ground plane is crucial for impedance matching, hence distance g_3 between the antenna and the ground plane is optimized through simulation. The tapered ground plane limits stray electric field and parasitic capacitance and yields better impedance matching at higher frequency. Among various parameters, OSRR split gaps g_3, g_4, and g_5, ground length G_2, and the gap between OSRR and feedline g_1 have phenomenal impact on the reflection coefficient. The validation of the proposed design is done using a fabricated prototype. Figure 3(a) illustrates the fabricated antenna. The antenna parameters are measured in an anechoic chamber which is furnished in Figure 3(b). Figure 3(c) depicts the simulated and tested S_{11} plots of the proposed design. The antenna exhibits its foremost resonance at 2.675 GHz with a measured impedance bandwidth of 425 MHz. The second resonance is measured at 3.45 GHz with

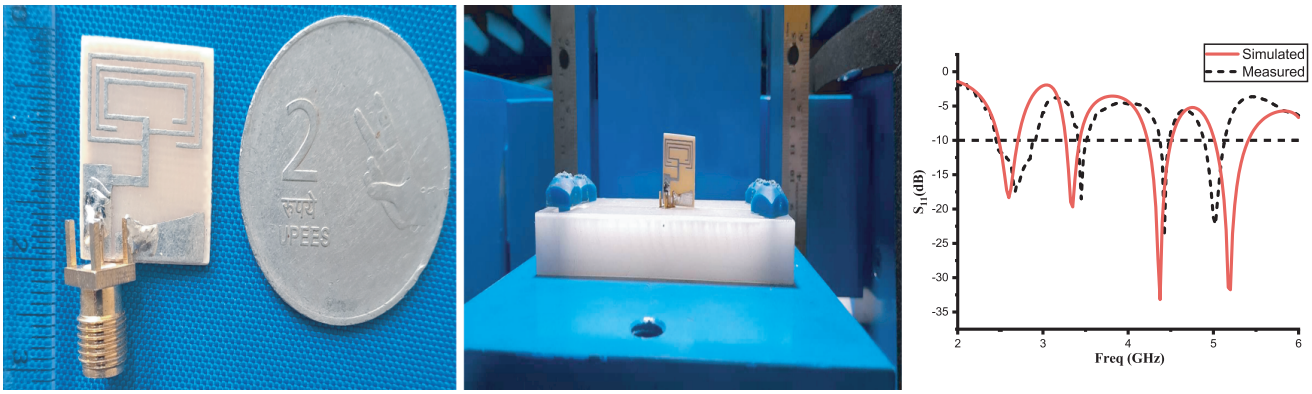

(a) (b) (c)

Figure 3. (a) Fabricated prototype. (b) Antenna measurement setup in anechoic chamber. (c) Simulated and Measured S_{11} plot.

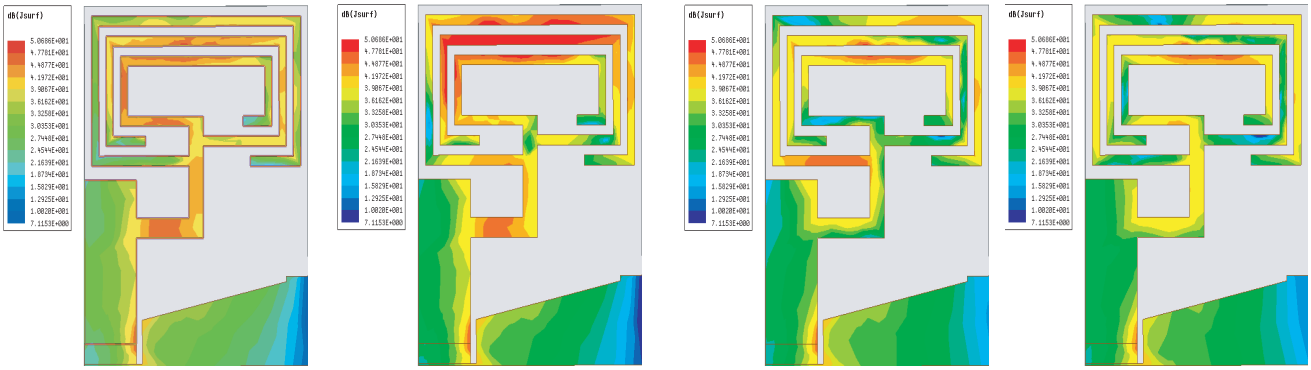

(a) (b) (c) (d)

Figure 4. Simulated current distribution at (a) 2.64 GHz, (b) 3.36 GHz, (c) 4.38 GHz, (d) 5.2 GHz.

an impedance bandwidth of 100 MHz, third resonance at 4.425 GHz with an impedance bandwidth of 125 MHz, and the fourth resonance at 5.02 GHz with impedance bandwidth of 225 MHz. The measured results are in fair equivalence with the simulated one. Slight variations between the two may be due to fabrication imperfections, connector losses, cable losses, scattering due to near field objects or errors in measurement. Figures 4(a)–4(d) depict the current distribution on antenna surface at all four operating frequencies. It is clear from Figure 4(a) that current is more predominantly distributed across the feedline and two inner rings of OSRR for 2.6 GHz. At 3.36 GHz, the current distribution is more at the feedline and three rings of OSRR. From this it is evident that these resonant frequencies may be attributed to the OSRR. At 4.38 GHz and 5.2 GHz, the current is evident at outer ring and inner ring, respectively, from which it is evident that OSRR is less resonant to higher frequencies. Thus from the current distribution it may be deduced that OSRR is more resonant at lower frequencies (2.6 GHz and 3.36 GHz) than at the higher frequencies (4.38 GHz and 5.2 GHz.) Figures 5(a)–5(h) demonstrate the simulated and tested radiation patterns at 2.64 GHz, 3.36 GHz, 4.38 GHz, and 5.2 GHz. For all the operating frequencies, the patterns are omnidirectional in the xz-plane and bidirectional in the xy-plane. Figure 5(i) and Figure 5(j) depict the three dimensional radiation pattern of antenna which exhibits an omnidirectional gain of 1.2 dBi and 2.3 dBi at 2.64 GHz and 3.36 GHz, respectively. Figure 5(k) illustrates the tested and simulated gain plots of the presented antenna. A gain of 1.2 dBi, 2.33 dBi, 2.75 dBi, 2.66 dBi is achieved at 2.64 GHz, 3.36 GHz, 4.38 GHz and 5.2 GHz, respectively, with an average gain of 2.24 dBi. Table 1 shows a comparison of the presented work with similar works from literature

in terms of size, operating frequency, type of antenna, gain achieved, type of feed, and bandwidth. Compared to other designs in literature, the proposed quad band ESA has a compact size and sufficient gain which makes it a suitable candidate for WiMAX and WLAN applications.

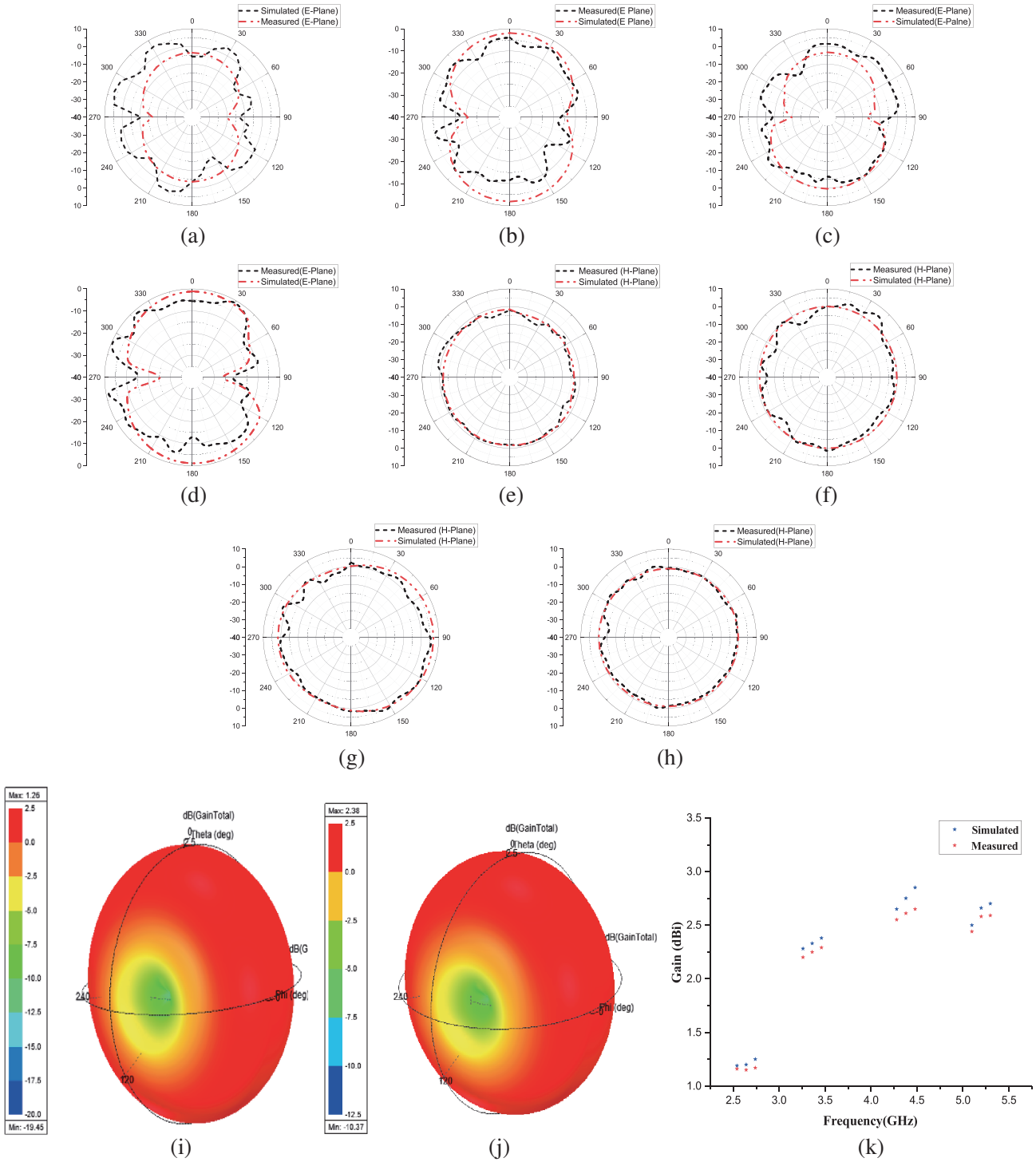

Figure 5. *E*-plane radiation pattern at (a) 2.64 GHz, (b) 3.36 GHz, (c) 4.38 GHz, (d) 5.2 GHz. *H*-Plane radiation pattern at (e) 2.64 GHz, (f) 3.36 GHz, (g) 4.38 GHz, (h) 5.2 GHz. (i) 3D radiation pattern at 2.64 GHz. (j) 3D radiation pattern at 3.36 GHz. (k) Gain plot of antenna.

Table 1. Comparison with other ESA in literature.

Reference	Physical Dimension ($L \times W$)	Frequency Covered	Antenna Type	Peak Gain	Type of Feeding	Bandwidth (MHz)
[14]	40 mm × 12 mm	2.45 GHz, 3.37 GHz	Dual Band	0.3/1.1	CPW	199 MHz/ 800 MHz
[15]	40 mm × 40 mm	3.04/3.83/ 4.83/5.76 GHz	Quad Band	2.36/1.43/ 2.11/2.39	CPW	25/25/ 39/41
[16]	18.5 mm × 22 mm	1.55/2.66/ 3.6/5.2 GHz	Quad Band	0.77/2.06/ 2.68/5.55	Asymmetric CPW	80/190/ 575/675
This work	18 mm × 15.5 mm	2.64/3.36/ 4.38/5.2 GHz	Quad Band	1.2/2.33/ 2.75/2.66	ACS	220/160/ 270/390

4. EXTRACTION OF NEGATIVE PERMEABILITY OF OSRR

Open SRR introduced as the radiator in this design is obtained by modifying the split dimensions of conventional SRR. With the aid of classical waveguide theory, the characteristics of the OSRR are analysed. Further, electromagnetic excitation is imparted along the input port, and S_{11} and S_{22} are measured from the output port for retrieving the negative permeability of OSRR. A much related environment is simulated using HFSS software wherein the simulated values of S_{11} and S_{22} are used to obtain permeability characteristics of OSRR. Figure 6(a) shows the experimental setup in which OSRR is placed in a waveguide medium in HFSS. The input and output ports are applied along x-axis. The perfect electric conductor boundary and perfect magnetic conductor boundary are applied along y- and z-axes, respectively. The OSRR unit cell is exposed to electromagnetic waves through port 1, and the corresponding S-parameters are retrieved from port 2. Those S-parameters are then used to obtain permeability making use of Nicholson Ross Weir equation [17]. Figure 6(b) illustrates the extracted real and imaginary parts of permeability of OSRR from which it is evident that both real and imaginary parts of the permeability of OSRR are negative at 3.78 GHz and 4.2 GHz. This is a confirmation to the presence of negative permeability characteristics in the proposed OSRR which enhances the overall performance of the proposed antenna. The higher order modes of OSRR are excited which enables the multiband functionality of the antenna.

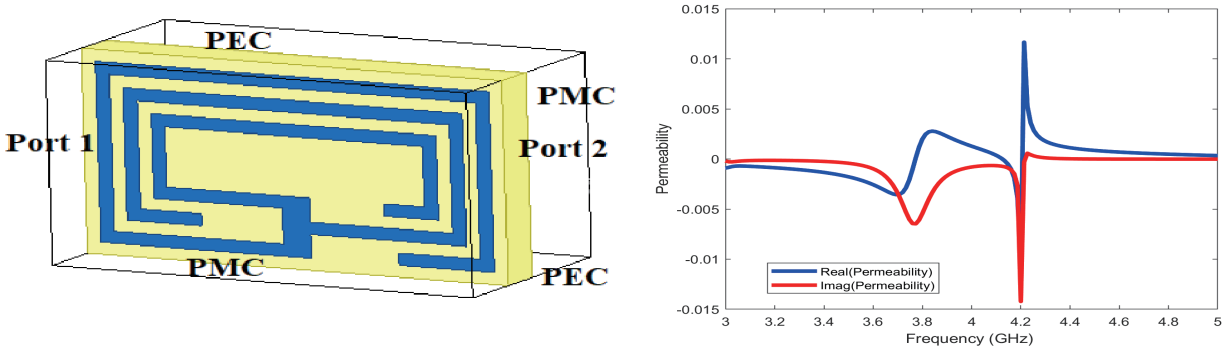

(a) (b)

Figure 6. Extraction of negative permeability of OSRR. (a) Waveguide setup of OSRR. (b) Real and imaginary part of extracted permeability.

5. CONCLUSION

A novel ACS-fed electrically small antenna is presented and validated for quad band operation. The proposed antenna operates at 2.64 GHz, 3.36 GHz, 4.38 GHz, and 5.2 GHz revealing an impedance bandwidth of 220 MHz, 160 MHz, 270 MHz, and 390 MHz, respectively. The antenna has a compact size of $0.136\lambda_0 \times 0.158\lambda_0 \times 0.014\lambda_0$ at 2.64 GHz with $ka = 0.65$. The metamaterial property of OSRR is affirmed through analysis. The proposed design achieves an average gain of 2.24 dBi. Thus the design puts forward an antenna with quad band operation and fair radiation properties suitable for WiMAX and WLAN applications.

REFERENCES

1. Wheeler, H. A., "Fundamental limitations of small antennas," *Proceedings of the IRE*, Vol. 35, No. 12, 1479–1484, 1947.
2. Davis, W. A., T. Yang, E. D. Caswell, and W. L. Stutzman, "Fundamental limits on antenna size: A new limit," *IET Microwaves, Antennas & Propagation*, Vol. 5, No. 11, 1297–1302, 2011.
3. Patel, R., A. Desai, and T. K. Upadhyaya, "An electrically small antenna using defected ground structure for RFID, GPS and IEEE 802.11 a/b/g/s applications," *Progress In Electromagnetics Research Letters*, Vol. 75, 75–81, 2018.
4. Erentok, A. and R. W. Ziolkowski, "Metamaterial-inspired efficient electrically small antennas," *IEEE Transactions on Antennas and Propagation*, Vol. 56, No. 3, 691–707, 2008.
5. Joshi, J. G., S. S. Pattnaik, S. Devi, and M. R. Lohokare, "Electrically small patch antenna loaded with metamaterial," *IETE Journal of Research*, Vol. 56, No. 6, 373–379, 2010.
6. Itoh, T. and C. Caloz, *Electromagnetic Metamaterials: Transmission Line Theory and Microwave Applications*, John Wiley & Sons, 2005.
7. Dalgaç, Ş., F. Karadağ, E. Ünal, V. Özkaner, M. Bakır, O. Akgöl, U. K. Sevim, et al., "Metamaterial sensor application concrete material reinforced with carbon steel fiber," *Modern Physics Letters B*, Vol. 34, No. 10, 2050097, 2020.
8. Pandeeswari, R., "SRR and NBCSRR inspired CPW fed triple band antenna with modified ground plane," *Progress In Electromagnetics Research C*, Vol. 80, 111–118, 2018.
9. Shobana, M., R. Pandeeswari, and S. Raghavan, "Design of sub-6 GHz antenna using negative permittivity metamaterial for 5G applications," *International Journal of System Assurance Engineering and Management*, 1–13, 2022.
10. Naidu, P. V., A. Kumar, and R. Rengasamy, "Uniplanar ACS fed multiband high-gain antenna with extended rectangular strips for portable system applications," *International Journal of RF and Microwave Computer-Aided Engineering*, Vol. 29, No. 10, e21870, 2019.
11. Naidu, P. and A. Malhotra, "Design & analysis of miniaturized asymmetric coplanar strip fed antenna for multi-band WLAN/WiMAX applications," *Progress In Electromagnetics Research C*, Vol. 57, 159–171, 2015.
12. Kang, L., et al., "Compact ACS-fed monopole antenna with rectangular SRRs for tri-band operation," *Electronics Letters*, Vol. 50, No. 16, 1112–1114, 2014.
13. Pillai, P. N. and R. Pandeeswari, "A compact uniplanar ACS-fed metamaterial inspired dual band antenna for S-band and C-band applications," *Applied Physics A*, Vol. 128, No. 4, 1–13, 2022.
14. Sharma, S. K., M. A. Abdalla, and R. K. Chaudhary, "An electrically small sicrr metamaterial-inspired dual-band antenna for WLAN and WiMAX applications," *Microwave and Optical Technology Letters*, Vol. 59, No. 3, 573–578, 2017.
15. Boukarkar, A., et al., "Miniaturized single-feed multiband patch antennas," *IEEE Transactions on Antennas and Propagation*, Vol. 65, No. 2, 850–854, 2016.
16. Ameen, M. and R. K. Chaudhary, "Quad-band electrically small dual-polarized ZOR antenna with improved bandwidth using single-split ring resonators and spiral slots enabled with reflector for GPS/UMTS/WLAN/WiMAX applications," *2019 URSI Asia-Pacific Radio Science Conference (AP-RASC)*, IEEE, 2019.

17. Arora, C., S. S. Pattnaik, and R. N. Baral, "Performance enhancement of patch antenna array for 5.8 GHz Wi-MAX applications using metamaterial inspired technique," *AEU — International Journal of Electronics and Communications*, Vol. 79, 124–131, 2017.